NWRI Independent Peer Review of SCCWRP's Coupled Regional Ocean Monitoring System and Biogeochemical Elemental Cycling Model

17–18 January 2024

Charge questions:

(1) Assess model readiness to answer management questions;

Research models vs. Operational Regulatory Models

(2) Advise on model uncertainty associated with addressing management questions;

(3) Recommend next steps for improving the model readiness

South Orange County Wastewater Authority

Topic: Evalution of SCCWRP Variant ROMS-BEC Model Source Code (particular process concerns)

By Scott Jenkins, Ph.D,

1) Evaluated ROMS/BEC codes including: 231 .F-codes written in Fortran 90 and 57 .h-header codes written in C; plus 131 Fortran 90 and numerous control files in G-code related to non-hydrostatic ROMS (aka, CROCO-NH). Hydrostatic-ROMS codes were written in *assembly language* and were unreadable.

2) Two Concerns about Process Omissions in these codes:
   * The formulation of light attenuation throughout the water column omits back-scattering
   * The schematization of the dilution of effluent discharges from ocean outfalls omits initial dilution occurring prior to diffuser jet merging and plume formation, and assumes a fixed, time-invariant mixing volume (which never occurs with effluent plumes in nature)

3) These omission impart a bias in the modeled results that over-stimulate algal photosynthetic rates, growth rates and NPP; while underpredicting dilution of outfall effluent

Concern #1: Omission of Scattering in the Formulation of Light Attenuation

Incident Light Attenuates with Depth due to Absorption ***and Scattering*** by Sea Water Molecules, Phytoplankton, Suspended Sediment/Particulate, and Dissolved Organic Matter, (DOM).

SCCWRP ROMS/BEC considers ONLY Absorption by Seawater and by Phytoplankton

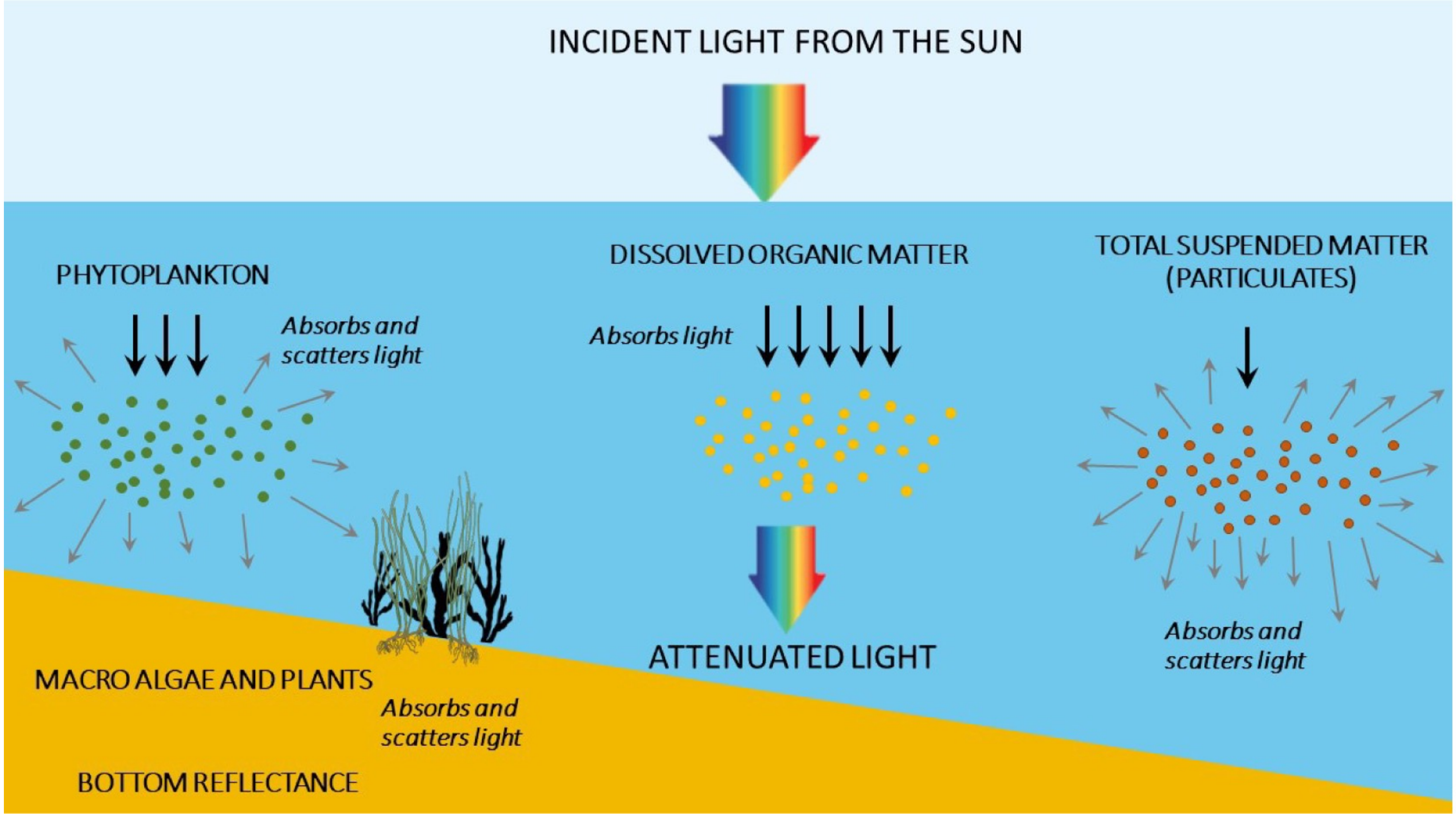

Concern #1: Omission of Scattering in the Formulation of Light Attenuation

Photosynthesis, phytoplankton growth rates, and biomass are controlled by the availability of nutrients and light at wave lengths between 400 nm and 700 nm, or photosynthetically available radiation, (*PAR*). Mie Theory teaches that PAR decays exponentially with depth, z , in the water column from a maximum level at the sea surface, *PARO,* according to:

$$PARz = PARO \exp\left[-C_d\, z\right]$$

where C_d is the *diffuse attenuation coefficient*. The complete representation of the *diffuse attenuation coefficient* is given by Morel and Loisel (1998) as:

$$C_d = \frac{a}{\cos\Omega}\left[1 + \frac{b}{aB_0}\int_0^{\theta} \beta(N,k,\theta)\,d\theta\right]^{0.5}$$

Where: $B_0 = \int_0^{\pi} \beta(N_0,k_0,\theta)\,d\theta$ is the total *volume scattering function* at the sea surface; Ω is the angle of down-welling light; a is the absorption coefficient; b is the scattering coefficient; and $\beta(k,N,\theta)$ is the *volume scattering function* of suspended particulate with non-dimensional particle diameter, $k = D/2\lambda$, where D is the physical particle diameter, and N is the particle number concentration (numbers of scattering and absorbing particles per unit volume); θ is the scattering angel.

Concern #1: Omission of Scattering in the Formulation of Light Attenuation

Curtis Deutsch and Hartmut Frenzel Formulation of PAR Attenuation with Depth

```
cff=deg2rad*latr(i,j)
        cos_Znt=cos_Thr*cos_dec*cos(cff)+sin_dec*sin(cff)
        if (cos_Znt.gt.0.) then
         PAR0=PAR0_ell*cos_Znt*(1.-ccf1+ccf2*cos_Znt)
    &       *(1.-cloud*( ccf3+ccf4*sqrt(1.-cos_Znt*cos_Znt)))
         do k=1,N                        ! From Eppley, d-1:
          Vp=0.851*1.066**t(i,j,k,nnew,itemp) !   Vp=2.9124317 at
                                         !   t=19.25 degrees
          PARz=PAR0*exp(-abs(z_r(i,j,k))*(kwater+kphyto*Phyt(k)))
```

Where:

Parameters as in Table 1; Fasham et al. [JMR, 48, 591-639, 1990]

```
!
    &   kwater = 0.04, ! light attenuation due to absorption by sea water [m-1]
    &   kphyto = 0.03, ! light attenuation due to absorption by Phytoplankton
                 !                  [(m^2 mMol N)-1]
```

Hence: kwater+kphyto* Phyt(k) = are actually just the absorption coefficient, and do not represent the total attenuation coefficient

Diffuse attenuation coefficient C_d in the PAR band for European waters, at 100m resolution. Dark blue/violet colors correspond to highest attenuation of PAR, ($C_d \sim 1.959$), while yellow colors Correspond to lowest attenuation of PAR, ($C_d \sim 0.045$), from Bekkby (2020)

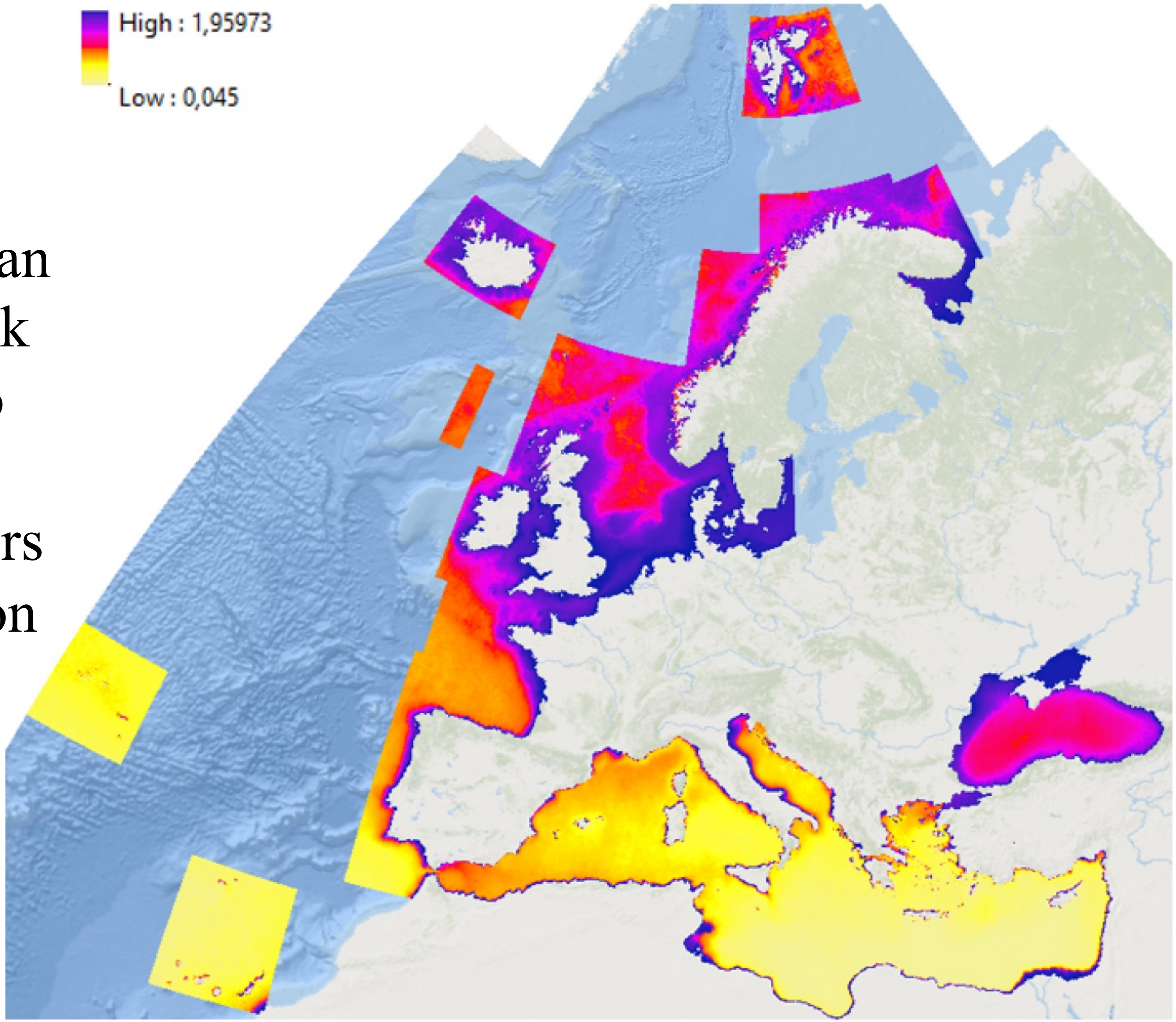

Scattering and Absorption of PAR due to Suspended Sediment from River Runoff

Suspended sediment contours (red) calculated by early Navy ROMS model overlaid on LANDSAT multi-spectral scanner image of wash load runoff from the Santa Margarita River at Oceanside, CA during the El Nino storm of 23 January 1993. Modeled suspended sediment concentrations expressed in base-10 log scale of particle number per ml. Colored patchwork denotes drainage basins of local secondary and tertiary streams and creeks. (from Hammond, et al., 1995)

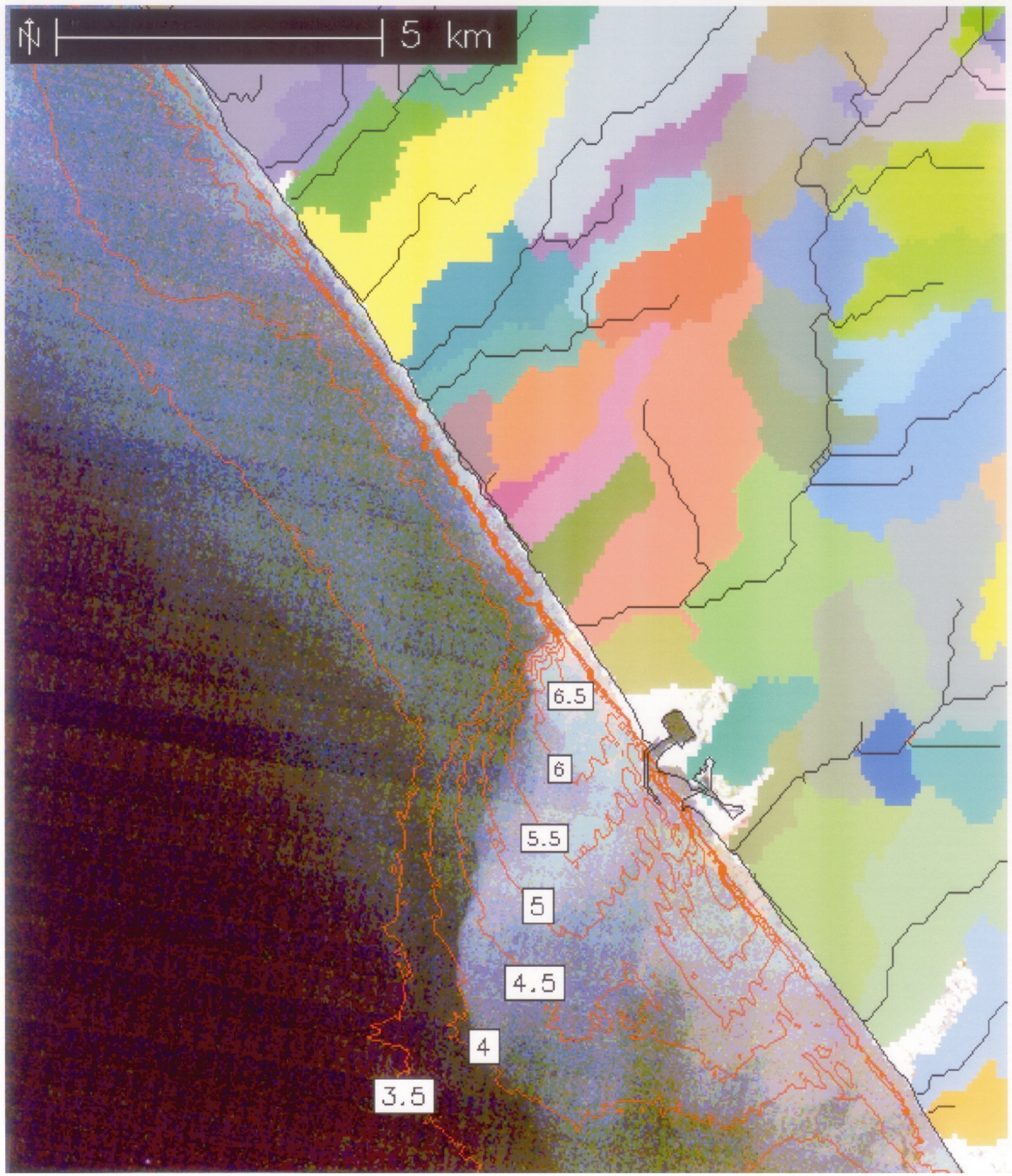

Measurements of Relative Strength of Scattering vs. Absorption in Coastal Waters

Measured scattering coefficients, *b*, (left) and absorption coefficients, *a*, (right) offshore of Oceanside, CA. Note scattering coefficients are more than 2-3 times greater than absorption coefficients across the PAR band,
(from Hammond et al., 1995)

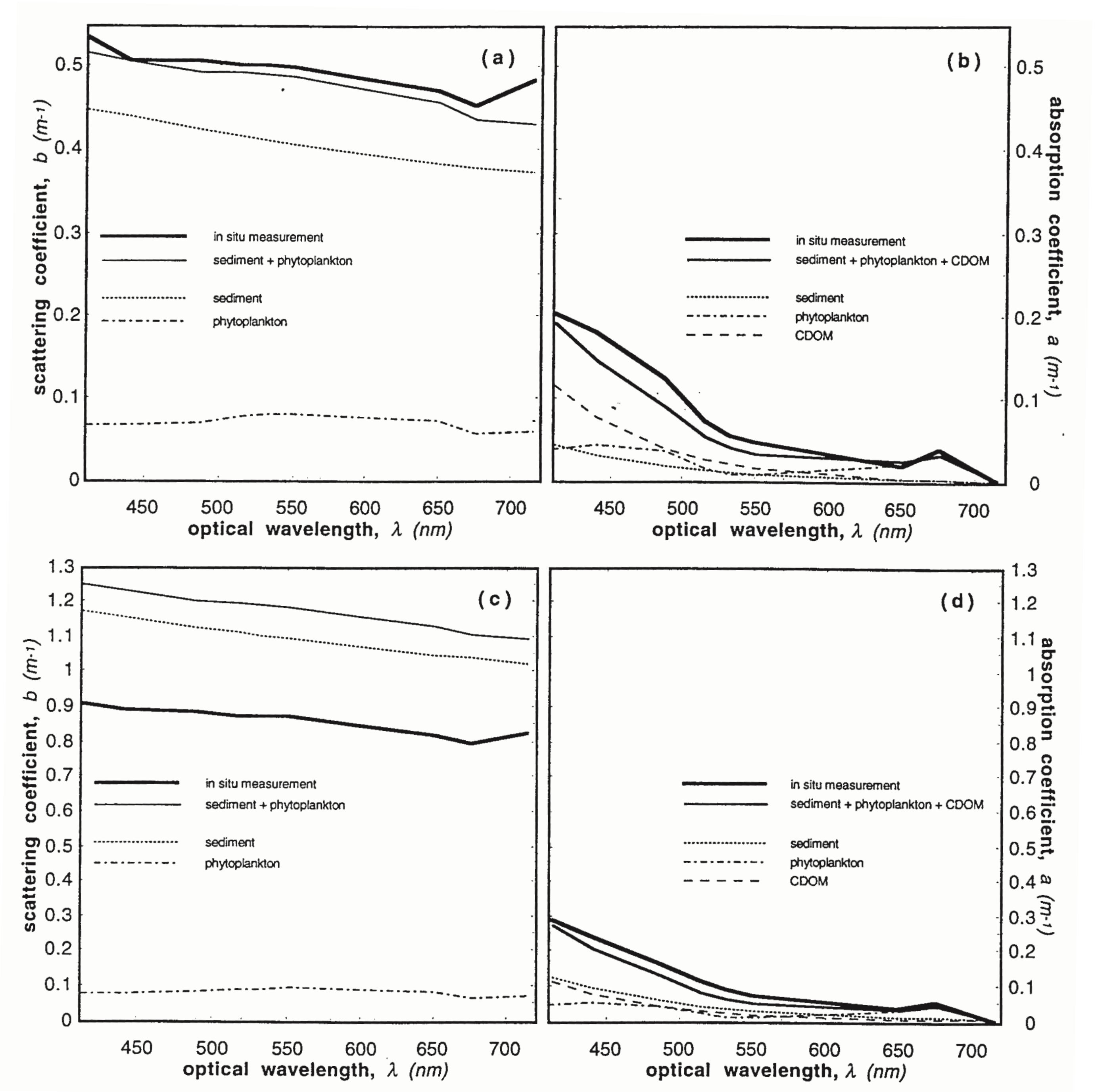

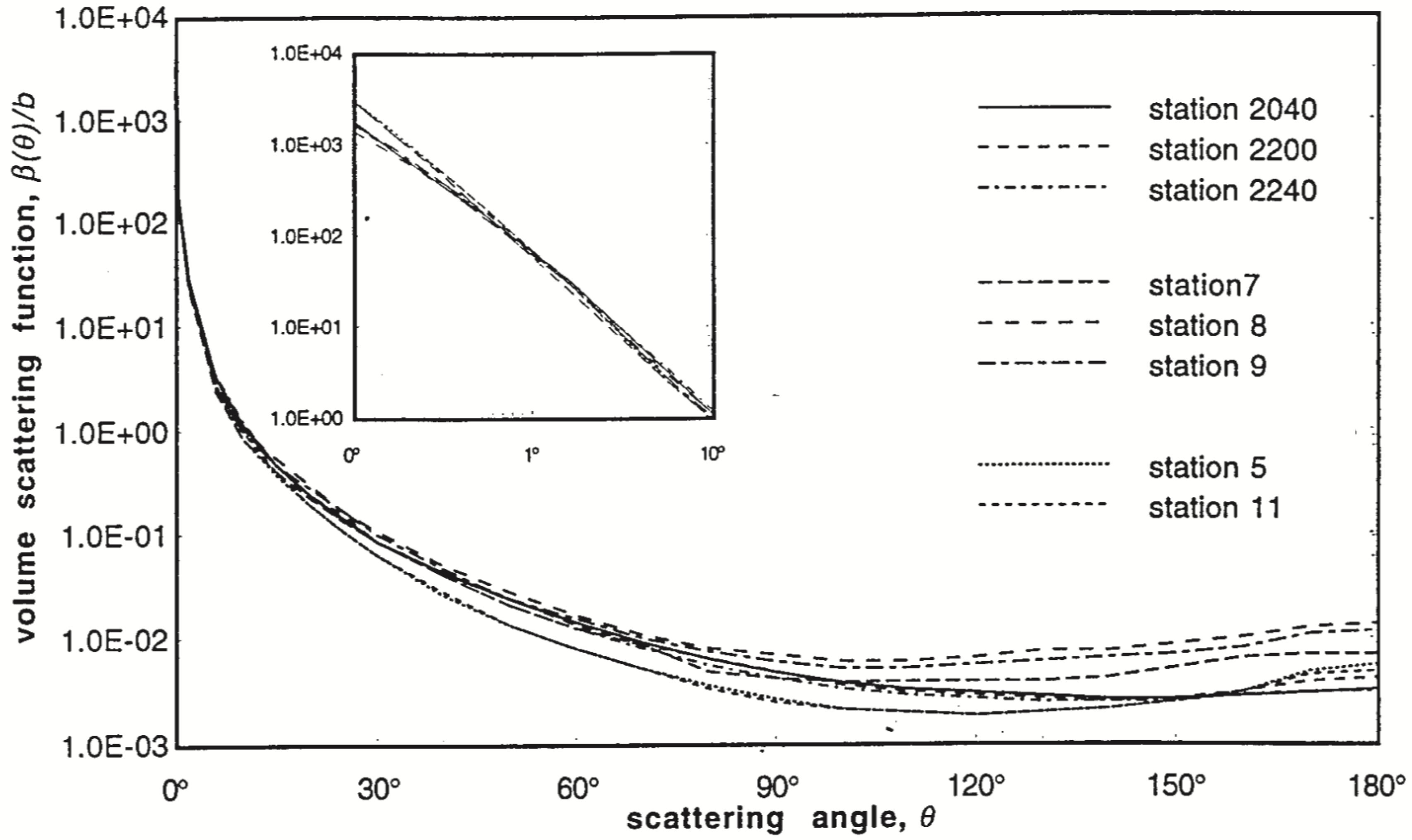

Volume Scattering Function in the PAR band, $\beta(N,k,\theta)$, at 8 sampling stations where water depths range from -10 m to - 80 m MSL, and 0.05 < k < 0.91 (from Hammond et al., 1995).

$$C_d = \frac{a}{\cos\Omega}\left[1 + \frac{b}{aB_0}\int_0^{\theta} \beta(N,k,\theta)\,d\theta\right]^{0.5}$$

$$k = D / 2\lambda$$

Settling Velocities of Suspended Sediment (from Sverdrup, et al., 1942)

	Particle Diameter	**Size Parameter**	**Time to Fall 10cm**				**Settling Velocity**
	(μm)	k_{530} *(μm)*	*(days)*	*(hours)*	*(minutes)*	*(seconds)*	*(m/day)*
clay	0.12	0.11	87	3	19		0.001
	0.25	0.23	21	18	50		0.004
	0.49	0.45	5	10	42		0.018
	0.98	0.91	1	8	41		0.074
	1.95	1.81		8	10		0.3
silt	3.9	3.9		2	2	32	1.2
	7.8	7.2			30	38	4.7
	15.6	14.5			7	40	18.8
	31.2	29			1	55	75.2
	62.5	58				29	301
very fine sand	125	116				8.3	1040
fine sand	250	232				2.7	

Concern #1: Omission of Scattering in the Formulation of Light Attenuation

The most aggressive PAR scattering and absorbing particulate can remain in suspension for months as they disperse coastal currents and will not simply settle out of suspension following major storm and flood events.

LANDSAT multi-spectral scanner image of suspended particulate across the Southern California Bight due to dispersion of river wash load particulate following a Pacific storm on 14 March 1975.

Solution #1: Omission of Scattering in the Formulation of Light Attenuation

Omission of scattering in the codes of the SCCWRP variant of ROMS/BEC will impart a bias in the modeled results that will result in deeper *Euphotic Zone* predictions and higher predicted *Photosynthetic* and *Plankton Growth Rates* than would otherwise likely occur in Nature. To correct this bias the codes must be expanded to solve the full set of Mie Scattering algorithms to obtain solutions for the scattering coefficient, *b*, and volume scattering function, $\beta(N,k,\theta)$. This will also require gathering additional data on suspended sediment (particle) concentrations and particle size distributions of the suspended sediment using a laser particle sizer.
These data should be acquired for both the offshore ocean background levels and the river discharges. The most efficient scattering and absorbing particles at PAR wave lengths are in the size regime of clay, dust and sub-micron particulate, for which the particle number concentration varies with particle diameter and depth according to a hyperbolic distribution (Bader, 1970; Kirk, 1983) given by:

$$N = f(D,z) = N_1(z)\, D^{-\gamma}$$

$N_1(z)$ is the particle number concentration in the smallest size decade, which varies with depth, and typically represents particle sizes in the range of 0.1 micron to 1.0 micron; while γ is the slope of the particle size distribution on a logarithmic sale

Concern #2: SCCWRP Schematization of Ocean Outfall Point-Source Discharges

*The nearfield vertical mixing in the buoyant plume from an ocean outfall occurs on a scale smaller than the grid resolution of the SCCWRP variant of ROMS/BEC (300 m). The fixed-grid hydrostatic architecture of ROMS/BEC is an assemblage of 2-D solutions stacked between the seabed and sea surface that has no vertical dynamics, and consequently is ill-suited to resolve the large local vertical velocities occurring in the plume of a prototype-scale ocean outfall.

* First work-around: the SCCWRP variant of ROMS/BEC imposes an assumed fixed, time-invariant mixing volume around the outfall which never occurs in Nature .The size and shape of the mixing volume is defined by 2 *shape functions,* one that specifies the horizontal footprint of the plume, and the other that specifies the vertical shape of the plume using a *Gaussian functional with 2 free parameters,* (cf. Kessouri et al., 2021; Uchiyama et al., 2014).

*The free parameters in the vertical shape function are assumed to be the same for all outfalls, an assumption that amounts to one size fits all outfalls, both large and small.

Concern #2: SCCWRP Schematization of Ocean Outfall Point-Source Discharges

*The shape functions that define the size and shape of the mixing volume in SCCWRP's ROMS/BEC model do not replicate the size and shape of outfall plumes in Nature;
the horizontal footprint of the outfall plume can not be confined to a fixed set of grid cells, and the vertical cross-section of a prototype outfall plume does not follow a Gaussian distribution (see next slide).

*The mixing volume of a prototypic scale outfall plume in Nature varies continuously over time in response to the vertical variations in temperature/salinity profiles, winds, waves, currents, discharge rates, diffuser length, and numbers & size of discharge port; none of which SCCWRP's ROMS/BEC formulation of the mixing volume can replicate or approximate.

Mixing Volume and Initial Dilution of a prototype scale ocean outfall varies continuously in response to changes in the water column temperature/salinity profiles, the outfall discharge rate, and ambient winds, waves and currents

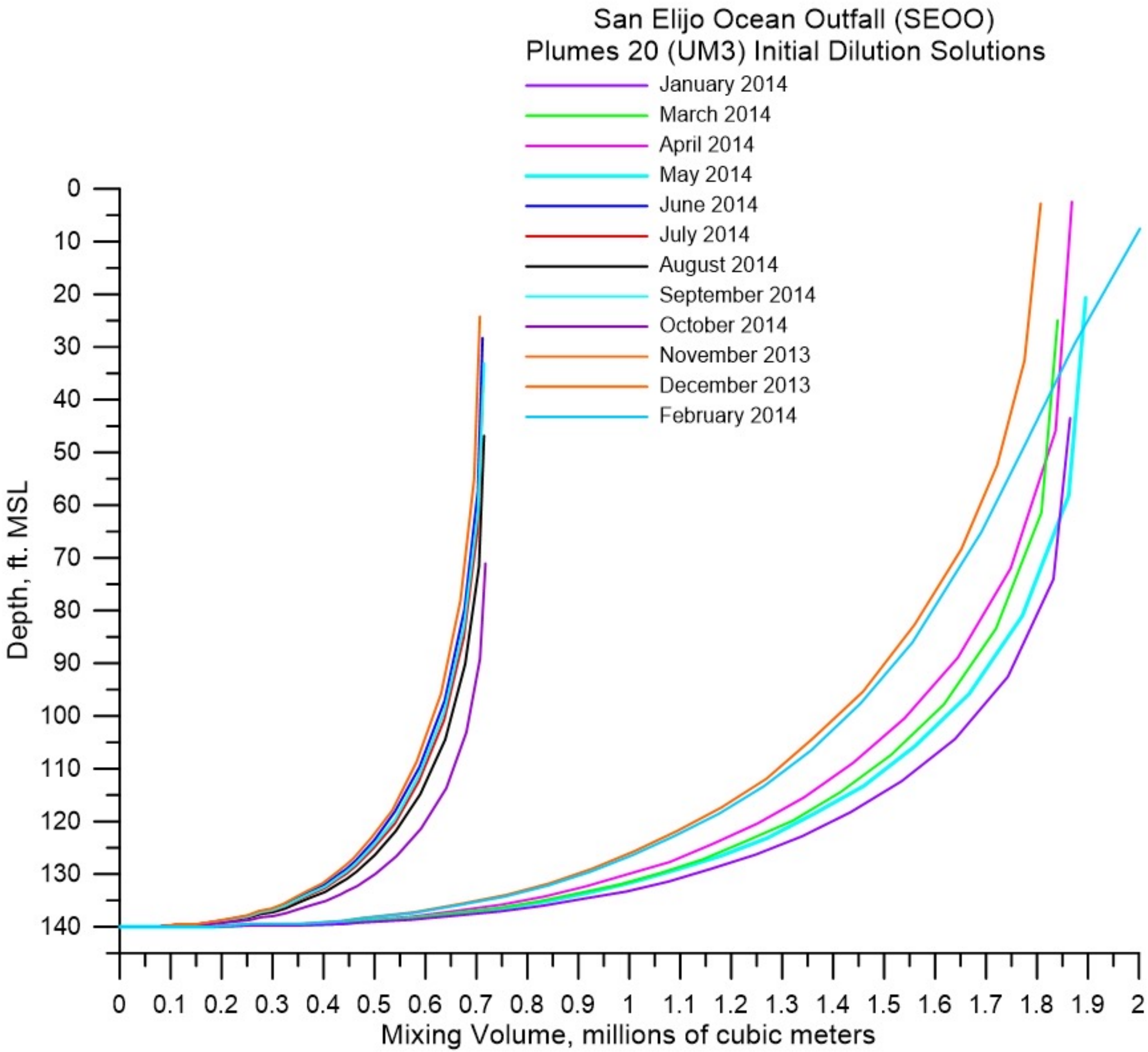

Concern #2: SCCWRP Schematization of Ocean Outfall Point-Source Discharges

*Second work-around, *Non-hydrostatic ROMS* (CROCO-NH): A nonhydrostatic discretization is applied locally to a small inner nested grid (3 km x 1.5 km x 60 m) creating an embedded singularity inside of the regional hydrostatic ROMS (Ho et al., 2021). No explicit eddy diffusivity parameterizations were used inside the embedded singularity, and as a result, the turbulence closure relations of ROMS are turned off.

*Inside the inner non-hydrostatic ROMS grid, the outfall discharge are represented as buoyant vertical fluxes through a line grid cells above the seabed. The calculated dilution results entirely from plume expansion driven by buoyancy convection.

*This schematization omits two processes that otherwise promote initial dilution

1) no initial dilution from ground effect by entrainment currents along the seabed
2) no initial dilution from turbulent jet entrainment prior to plume formation

*No source code was made available detailing what asymptotic matching formulations were used between the regional hydrostatic-ROMS and the embedded non-hydrostatic ROMS domains…source of numerical instabilities?

Concern #2: SCCWRP Schematization of Ocean Outfall Point-Source Discharges

*SCCWRP Application of non-hydrostatic ROMS to OCSD Santa Ana Outfall omits *ground effect,* i.e., the initial dilution by entrainment currents along the seabed produced turbulent jet diffusion prior to plume formation.

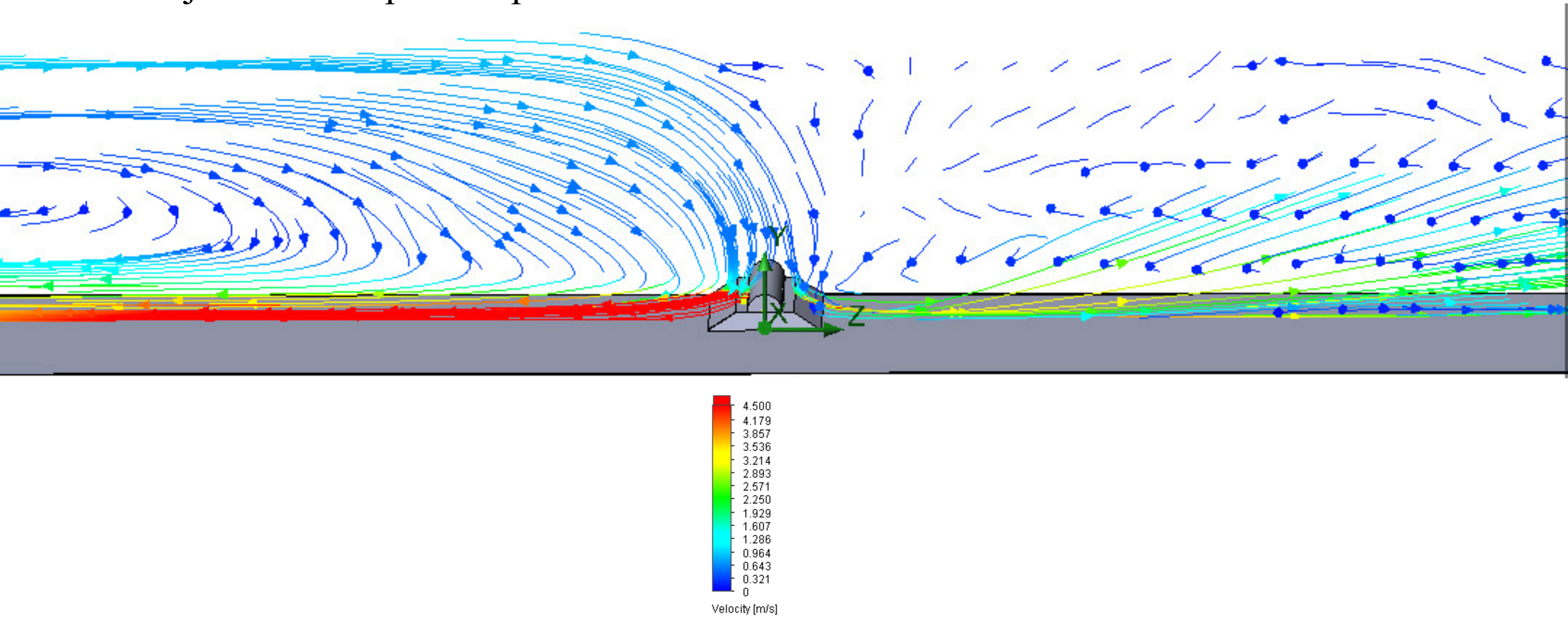

Concern #2: SCCWRP Schematization of Ocean Outfall Point-Source Discharges

*By either schematization, the SCCWRP variant of ROMS/BEC under predicts the dilution that occurs in the modeled outfall plume; which in turn, leads to higher undiluted nitrate and ammonia concentration in the plumes, thereby imparting a bias in favor of excessive plankton photosynthetic rates and growth rates stimulated by the exaggerated nutrient concentrations in both the nearfield and farfield of the outfall plumes.

*To correct this bias, the Plumes-20 (UM3) model can be incorporated within the present fixed grid hydrostatic architecture of hydrostatic ROMS/BEC by using it to recalculate the shape function of the mixing volume during each time step; thereby continually adjusting the size and shape of the mixing volume in response to changes in temperature/salinity profiles, discharge rates, wind, waves and currents. The size of the mixing volume is directly proportional to the dilution factor, and this amendment should solve the present issue of under-predicting outfall dilution

Concern #2: SCCWRP Schematization of Ocean Outfall Point-Source Discharges

Evidence is emerging that nutrients discharged from ocean outfalls in the lower SCB dilute much faster in the nearfield of the outfalls than the SCCWRP variant of ROMS/BEC predicts

Full depth contour plot (aka, heat map) of AUV measurements of fDOM during surveys of the discharge plume from Encina Ocean Outfall during ebb tide on 20 December 2021. Average EOO discharge rate =31.20 mgd during ebb tide; End-of-pipe discharge concentration of fDOM = 217.5 ppb (QSU); Mean ebb tide current = 0.304 m/s (0.59 kts) toward the southeast

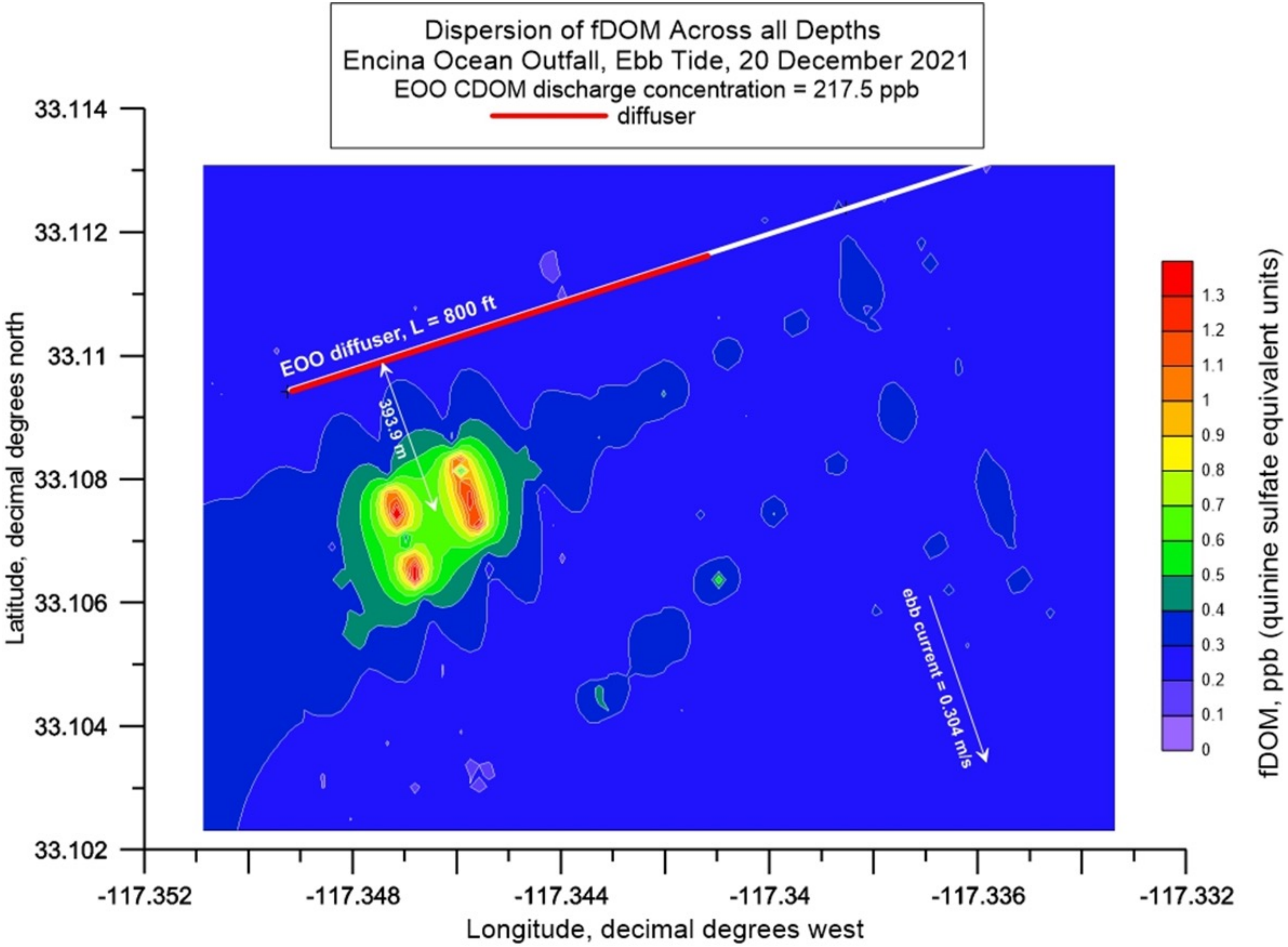

Concern #2: SCCWRP Schematization of Ocean Outfall Point-Source Discharges

Evidence is emerging that nutrients discharged from ocean outfalls in the lower SCB dilute much faster in the nearfield of the outfalls than the SCCWRP variant of ROMS/BEC predicts

Full depth contour plot (aka, heat map) of dilution factor derived from AUV measurements of fDOM during surveys of the discharge plume from Encina Ocean Outfall during ebb tide on 20 December 2021. Average EOO discharge rate =31.20 mgd during ebb tide; End-of-pipe discharge concentration of fDOM = 217.5 ppb (QSU); Mean ebb tide current = 0.304 m/s (0.59 kts) toward the southeast

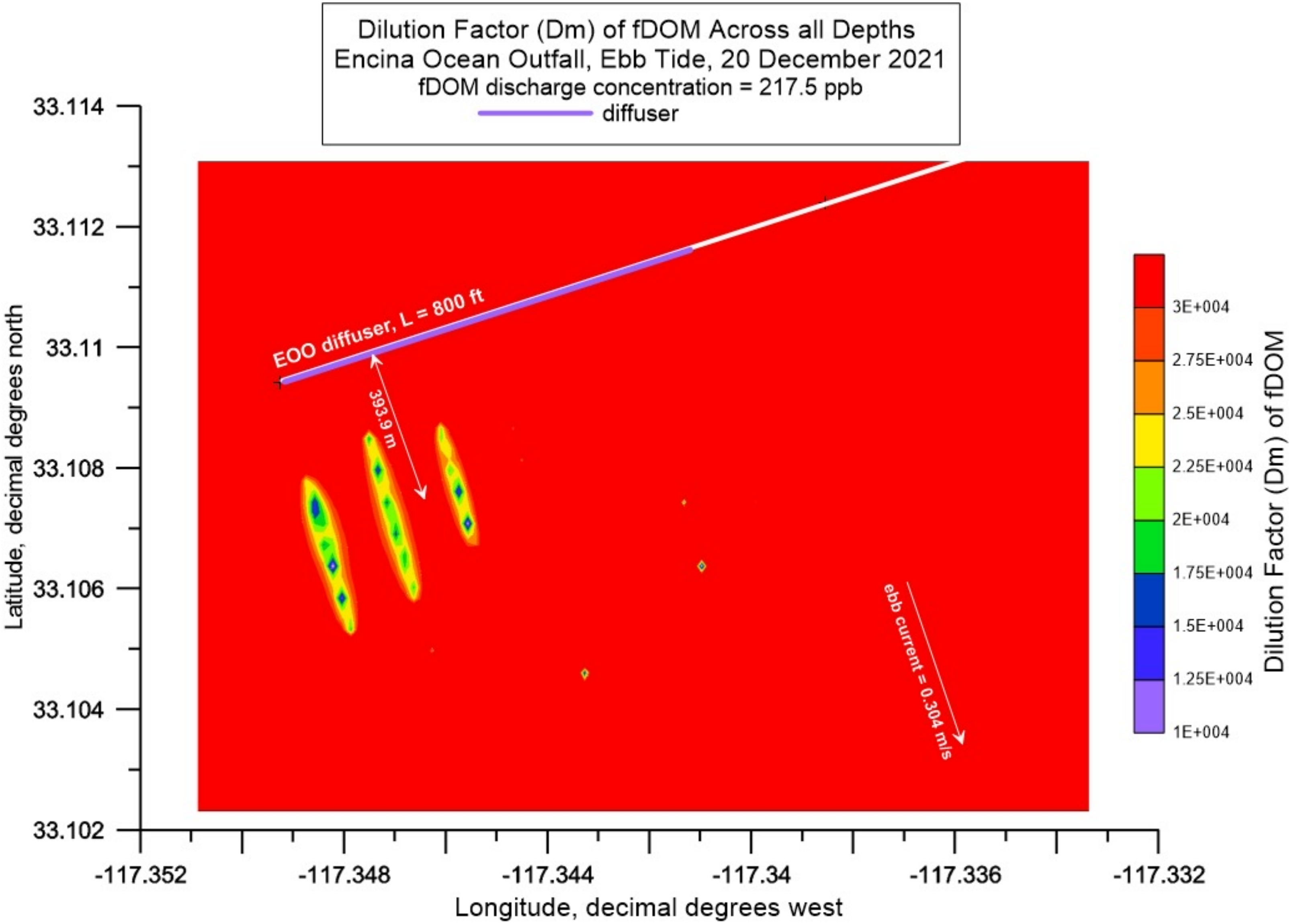

Concern #3: Possible CFL Instability at Reduced Grid Scales

*The embedded singularity imposed by the fixed mixing volume around the outfalls in the SCCWRP variant of ROMS/BEC could create numerical instabilities in the nutrient dispersion and plankton growth simulations.

*In order for the ROMS/BEC model to produce temporally stable solutions, the longest time step interval, Δt that can be used is limited by the Courant-Friedricks-Lewy (CFL) Stability Criteria:

$$\Delta t \leq \frac{\Delta x}{\sqrt{2gh}}$$

where Δx is the grid cell horizontal dimension, h is the depth of the seabed, and g is the acceleration of gravity. Hydrostatic ROMS uses a third-order upwind advective correction with hyper-diffusivity to suppress CFL instabilities. This approach often produces spurious mixing that increases over bottom gradients as grid resolution is made finer (Marchesiello, et al., 2009)

Concern #3: Possible CFL Instability at Reduced Grid Scales

Are the fine features in the third panel on the right-hand side of Figure-2 of Kessouri et al., (2021) run at time step intervals of 30 s factual or simply CFL instabilities? At horizontal grid resolution of $\Delta x = 300$ m, ROMS/BEC would have to run at time steps no longer than $\Delta t \leq$ 8 to 9 sec to avoid CFL numerical instabilities around the predominant outfalls neighboring the Palos Verdes Peninsula, (e.g., Hyperion or OCSD Santa Ana).

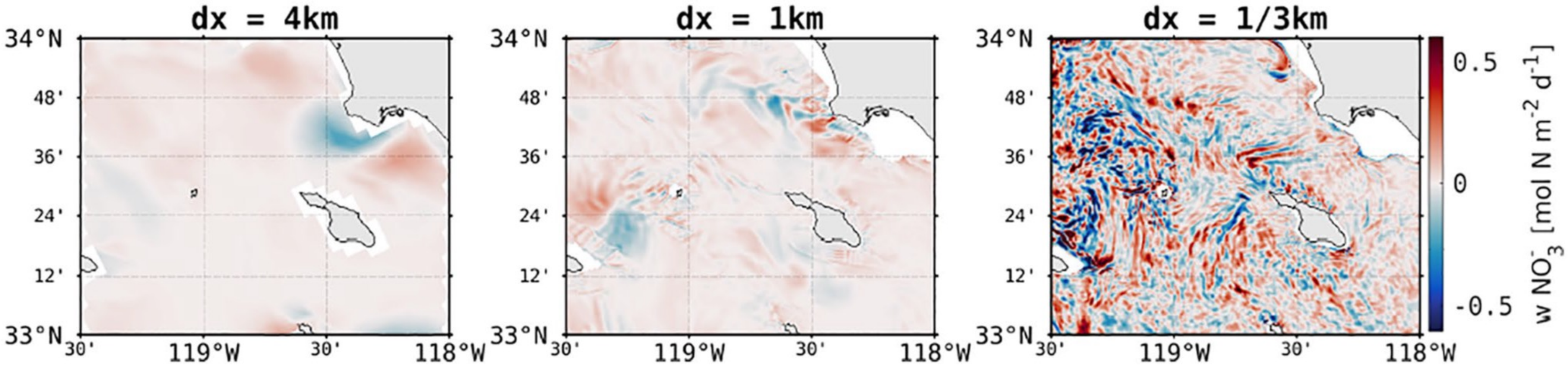

Figure 2. (Upper panel) Time series (1997–2001) of the vertical eddy flux of nitrate at 40-m depth calculated as follows $\overline{wN} = \overline{w}\,\overline{N} + \overline{w'N'}$, where the overbar represents a monthly average, and the prime the deviation from this average, for region covering the entire Southern California Bight (31.4°–35.3°N and 116.5°–121.8°W). The minimum and maximum values (i.e., the envelope) of the flux are shown in blue for the 4-km solution, in red for the 1-km solution, and in green for the 1/3 km. (Lower panel) Snapshot of the vertical flux of nitrate in spring at 40-m off the coast of Palos Verdes that shows higher magnitudes and enhanced variability as resolution increases.

Sensitivity of Model to Free Parameter Choices

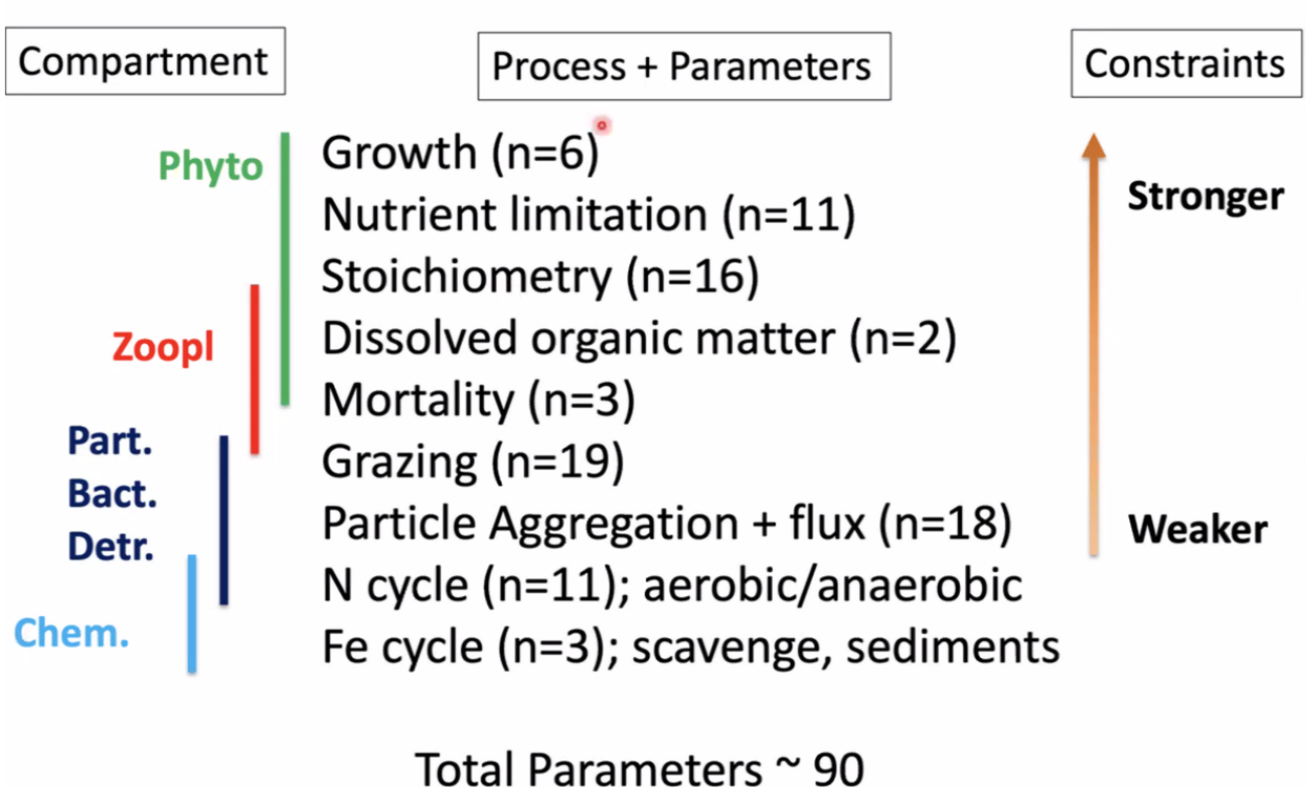

- A sensitivity analysis involving all possible combinations of 90 free parameters would involve 90! outcomes, (90! = 1.485716 X 10^{138}).

- Sensitivity analyses involving critical rate parameters that throttle non-linear functions should be performed & published in order to adequately address Charge Question (2); e.g. diffuse attenuation coefficient (both absorption & scattering); Michaelis-Menton half-saturation coefficients, mixing volume shape coefficients)

Sensitivity to parameter choices of rate constants of non-linear processes: Growth rate vs choice of *Michaelis-Menton half-saturation coefficient*

Parameterization: Nutrient→Growth

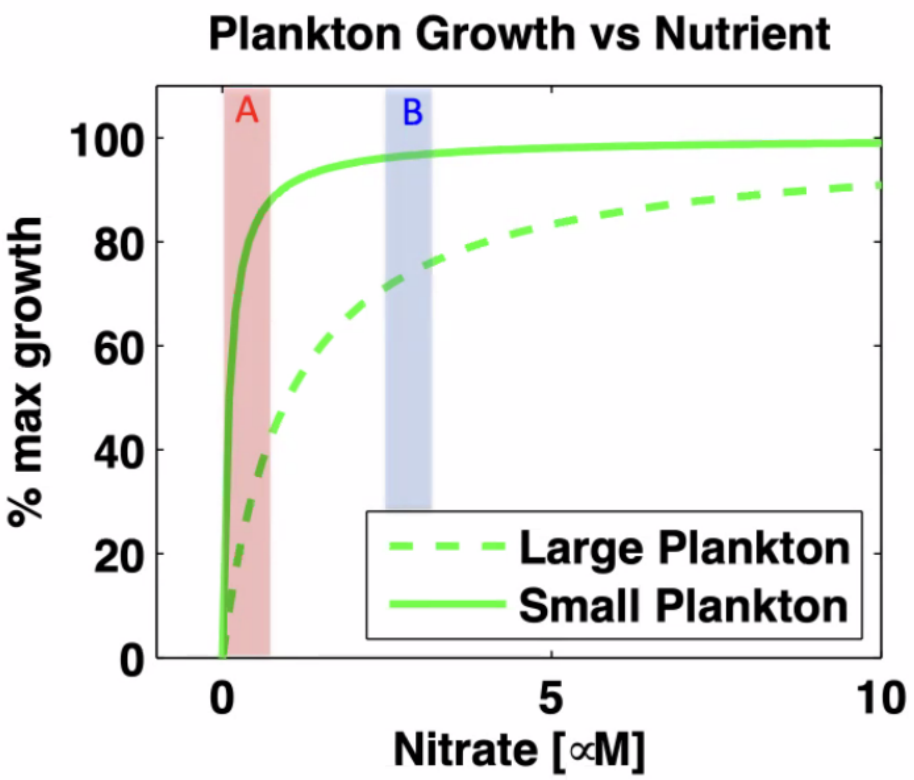

Growth rate dependence on nutrient is parameterized using Michaelis-Menten function. Basis in enzyme kinetics, parameters from lab studies.

Non-linear Biogeochemical responses. The response to perturbation depends strongly on the background state of the ocean before perturbation.

A: Nutrient increase over a low background level has a large impact, especially for small plankton.

B: Nutrient increase over a background level has a smaller impact, especially for large, fast-sinking plankton.

Sensitivity to parameter choices of rate constants of non-linear processes: Light attenuation & depth of Chlorophyll maximum vs choice of diffuse attenuation *coefficient (absorption + scattering)*

Nutrient vs Light Limitation

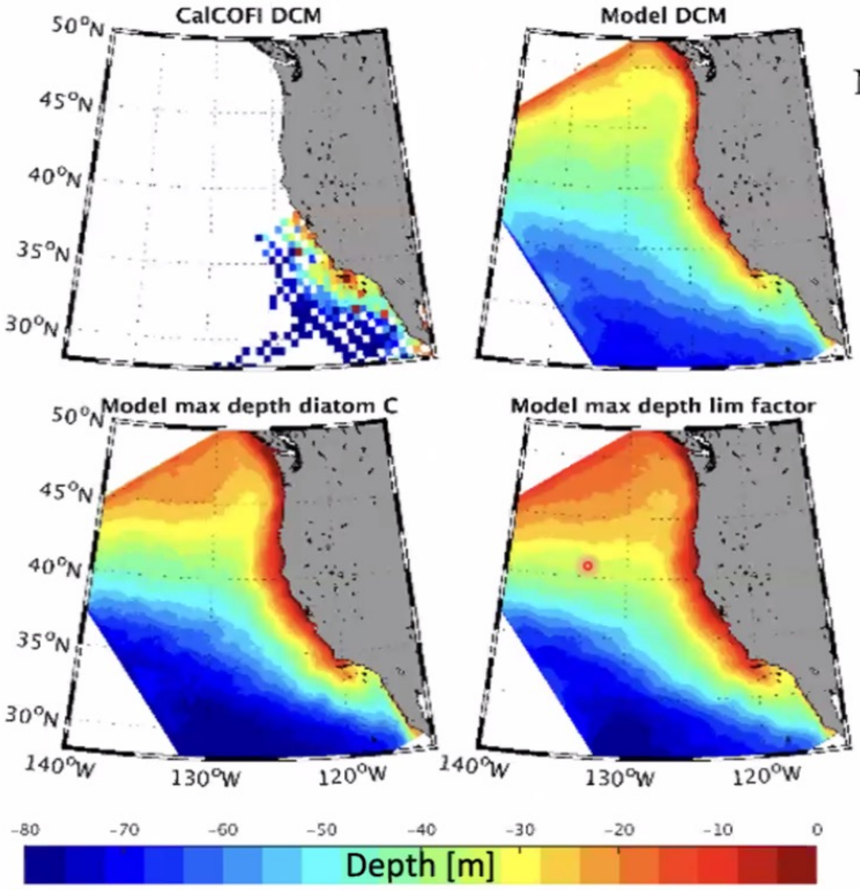

$$NPP = \Sigma_j \{\mu_{max} * \gamma_j (I) * min(\lambda(N_{i,j})) * B_j\}$$

Depth of the vertical maximum of Chlorophyll Reflects the trade-off between light (high at surface) and nutrients (high at depth).

Model fidelity to observations implies the model captures a realistic trade-off between nutrient limitation and light limitation.